

# Coupling of a metasurface with two non-coplanar and inter-perpendicular graphene nanoribbon arrays

Feng Chao Ni,<sup>1</sup> Ze Tao Xie,<sup>1</sup> Qi Chang Ma,<sup>1</sup> Jin Tao,<sup>3</sup> Jian Li,<sup>1</sup> Hongyun Meng,<sup>2</sup>  
and Xu Guang Huang<sup>1,2</sup>

<sup>1</sup> Guangzhou Key Laboratory for Special Fiber Photonic Devices and Applications, South China Normal University, Guangzhou 510006, People's Republic of China

<sup>2</sup> Provincial Key Laboratory of Nanophotonic Functional Materials and Devices, South China Normal University, Guangzhou 510006, People's Republic of China

<sup>3</sup> State Key Laboratory of Optical Communication Technologies and Networks, Wuhan Research Institute of Posts Telecommunications, Wuhan 430074, People's Republic of China

Author e-mail address: [huangxg@scnu.edu.cn](mailto:huangxg@scnu.edu.cn)

**Abstract:** A graphene metasurface is proposed and investigated. Through the analysis of the light field, the formation mechanism of the spectral splitting is attributed to the coupling between localized and delocalized graphene surface plasmon polaritons.

**OCIS codes:** (240.6680) Surface plasmons; (160.3918) Metamaterials; (130.3120) Integrated optics devices.

## 1. Introduction

Graphene has become an attractive alternative candidate for plasmonic material in terahertz and mid-infrared frequencies due to its unique physical properties [1]. Graphene has well-known properties including dynamical tunability and strong local field enhancement. The appearance of graphene has created a broader platform for the study of surface plasmon optoelectronics devices [2]. In this paper, we propose a design of metasurface with two non-coplanar and inter-perpendicular graphene nanoribbon arrays. The formation of an obvious spectral splitting is investigated: the coupling between localized and delocalized graphene surface plasmon polaritons giving rise to the induced dip.

## 2. Simulation Model

Under the condition of the random-phase approximation, the dynamical optical response of graphene can be calculated from the Kubo equation, its complex surface conductivity is estimated as [3]:

$$\sigma = \frac{e^2}{4\hbar} \left\{ \frac{1}{2} + \frac{1}{\pi} \arctan \left( \frac{\hbar\omega - 2E_f}{2k_B T} \right) - \frac{i}{2\pi} \ln \left( \frac{(\hbar\omega + 2E_f)^2}{(\hbar\omega - 2E_f)^2 + (2k_B T)^2} \right) \right\}, \quad (1)$$

$$+ \frac{2ie^2 k_B T}{\pi \hbar^2 (\omega + i\tau^{-1})} \ln \left( 2 \cosh \left( \frac{E_f}{2k_B T} \right) \right)$$

here  $\hbar$  is the reduced Planck's constant,  $\omega$  is the optical angular frequency,  $k_B$  is the Boltzmann constant,  $T$  is ambient temperature, and  $\tau$  is the carrier relaxation time.

The designed structure is shown in Fig. 1(a). An electrode substrate is sandwiched between two same-thickness layers of insulating medium. The periodic graphene nanoribbons arrayed in  $y$  direction are deposited on the top layer of insulating medium, while the periodic graphene nanoribbons

arrayed in  $x$  direction are deposited on the bottom layer of insulating medium. All of graphene nanoribbons in the two planes are composed of 5 graphene layers, to enhance the modulation depth [4]. The refractive index of the insulating medium and the electrode substrate are set to 1.45 and 4, respectively. An  $x$ -polarized normally incident plane wave along with the  $-z$  direction is utilized to excite the graphene plasmon on top layer of graphene nanoribbons. The 3D finite-difference time-domain (FDTD) method (Lumerical FDTD solutions software) is used to simulate of the unit cell structure.

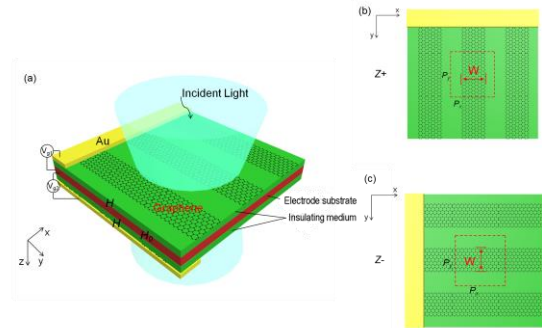


Fig. 1. (a) 3D schematic of the proposed structure. The thickness of electrode substrate  $H_0=10$  nm, and thickness of the insulating medium layers are both  $H$ . (b) The unit cell structure of our design on top layer, the periods of the  $x$  and  $y$  directions are  $P_x = 300$  nm and  $P_y = 300$  nm, respectively. Graphene nanoribbons width  $W = 150$  nm. (c) The unit cell structure of our design on bottom layer, the periods of the  $x$  and  $y$  directions are  $P_x = 300$  nm and  $P_y = 300$  nm, respectively. Graphene nanoribbons width  $W = 150$  nm.

## 3. Results and Discussions

In the simulations, Fermi level  $E_f$  of the graphene nanoribbons is set to be 0.5 eV, with the carrier relaxation time of  $\tau = 0.33$  ps and ambient temperature of  $T = 300$  K. Thicknesses of two insulating medium layers are both 40 nm. From the transmission spectrum of only top layer of graphene nanoribbons, a clear dip can be observed at  $5.33 \mu\text{m}$ , resulting from the SPPs resonant mode of the graphene nanoribbons

excited by the  $x$ -polarization incident light. However, for only bottom layer of graphene nanoribbons, the transmittance reaches about 1.0, because the SPPs mode of the graphene nanoribbons cannot be excited. Then we simulate and analysis the metasurface with double layers of graphene nanoribbons. The transmission spectrum displays an obvious spectral splitting with the main dip at  $5.47\ \mu\text{m}$  wavelength and the induced secondary dip at  $4.87\ \mu\text{m}$ , compared to the green dash line. Furthermore, a transmission peak appears at  $5.05\ \mu\text{m}$ . The result reveals that the two inter-perpendicular graphene nanoribbon arrays in different planes have been coupled each other to produce new a mode.

To explore the physics of the observed spectral splitting, we simulated respectively the field distributions of  $|E_z|^2$ -component corresponding to the main dip, the transmission peak and the secondary dip for  $H = 60\ \text{nm}$ . As shown in Fig. 3(a), only the SPPs on the top layer of graphene nanoribbons can be excited at  $\lambda = 5.26\ \mu\text{m}$ . Its light field concentrates mostly on the edges of the graphene nanoribbons and distributes along the  $\pm z$  directions, corresponding to the position of the main dip, while the bottom graphene nanoribbons have nearly no field distribution. One can see in Fig. 3(b) that the plasmonic resonance of the bottom graphene nanoribbons becomes pronounced at  $\lambda = 4.90\ \mu\text{m}$  and its light field is slightly overlapped with the one on the top graphene nanoribbons. In Fig. 3(c), at  $\lambda = 4.83\ \mu\text{m}$ , the plasmonic resonance of the bottom graphene nanoribbons becomes much stronger than that of the top graphene nanoribbons. As a result, the secondary dip at  $\lambda = 4.83\ \mu\text{m}$  is induced, as shown in Fig. 2(b). Additionally, Fig. 3(d) shows the field distribution of the  $E_z$ -component in the  $xoz$  plane at  $\lambda = 4.83\ \mu\text{m}$ . The  $E_z$  field distribution exhibits an antisymmetric form and excites a new mode of graphene nanoribbons.

Fig. 4 shows the  $E_z$  field distributions of the two graphene arrays in the  $x$ - $o$ - $y$  plane at  $\lambda = 4.83\ \mu\text{m}$ . The monitor in Fig. 4(a) is set at  $2\ \text{nm}$  above the top graphene nanoribbons arrayed in the  $y$ -direction, while the other monitor is set at  $2\ \text{nm}$  above the bottom graphene nanoribbons arrayed in the  $x$ -direction. It can be seen in Fig. 4(a) that the localized and anti-symmetric SPPs are excited in the top nanoribbon array, which has the largest intensity at nanoribbon boundaries. However, the  $E_z$  field of the bottom graphene nanoribbon array in Fig. 4(b) is the delocalized and symmetric SPPs boundary mode, propagating in the  $x$ -direction.

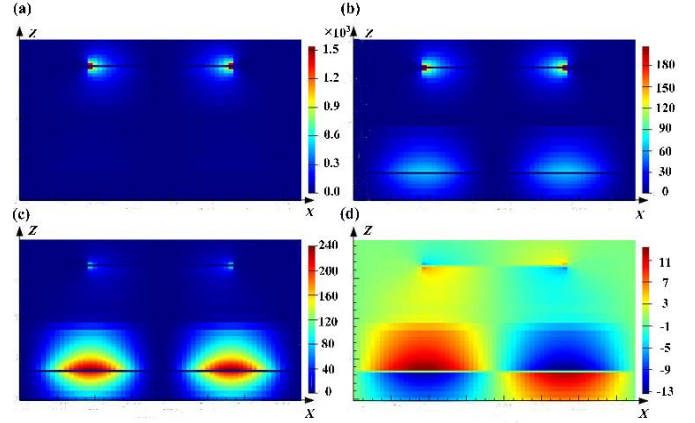


Fig. 3. The field distributions of the  $|E_z|^2$ -component at the main dip of  $5.26\ \mu\text{m}$  (a), the transmission peak of  $4.90\ \mu\text{m}$  (b) and the induced dip of  $4.83\ \mu\text{m}$  (c), for the thickness of the  $\text{SiO}_2$  of  $H = 60\ \text{nm}$ . (d) The  $E_z$  field distribution in the  $xoz$  plane at the wavelength of  $4.83\ \mu\text{m}$ .

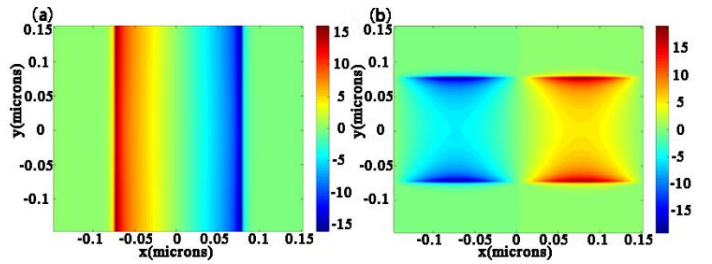


Fig. 4. The  $E_z$  field distributions of the two graphene arrays in the  $x$ - $o$ - $y$  plane for  $\lambda = 4.83\ \mu\text{m}$ . (a) The monitor is set at  $2\ \text{nm}$  above the top graphene nanoribbons arrayed in the  $y$ -direction. (b) The monitor is set at  $2\ \text{nm}$  above the bottom graphene nanoribbons arrayed in the  $x$ -direction.

#### 4. References

- [1] F. Wang, Y. Zhang, C. Tian, C. Girit, A. Zettl, M. Crommie, and Y. R. Shen, "Gate-variable optical transitions in graphene," *Science* 320(5873), 206–209 (2008).
- [2] J. Tong, M. Muthee, S.Y. Chen, S. K. Yngvesson, and J. Yan, "Antenna enhanced graphene THz emitter and detector," *Nano Lett.* 15(8), 5295–5301 (2015).
- [3] J. Lao, J. Tao, QJ. Wang, and XG. Huang, "Tunable graphene - based plasmonic waveguides: nano modulators and nano attenuators," *Laser Photonics Rev.* 8(4), 569–574 (2014).
- [4] H.-S. Chu and C. How Gan, "Active plasmonic switching at mid-infrared wavelengths with graphene ribbon arrays," *Appl. Phys. Lett.* 102(23), 231107 (2013).